

Syntheses and Characterization of Dicarbonyl–Nitrosyl Complexes of Technetium(I) and Rhenium(I) in Aqueous Media: Spectroscopic, Structural, and DFT Analyses

Roger Schibli,^{*,†,‡} Niklaus Marti,[†] Patrick Maurer,[†] Bernhard Spingler,[§] Marie-Line Lehaire,[†] Volker Gramlich,^{||} and Charles L. Barnes[⊥]

Center for Radiopharmaceutical Science, ETH-PSI-USZ, Paul Scherrer Institute, 5232 Villigen PSI, Switzerland, Department of Chemistry and Applied Biosciences ETH, 8093 Zurich, Switzerland, Department of Chemistry, University of Missouri—Columbia, Columbia, Missouri 65211, Laboratory of Crystallography ETH, 8092 Zurich, Switzerland, and Institute of Inorganic Chemistry, University of Zurich, 8057 Zurich, Switzerland

Received March 26, 2004

This work describes new synthetic routes to produce mixed carbonyl–nitrosyl complexes of technetium(I) and rhenium(I) in aqueous media. NaNO_2 , NOHSO_4 , and $\text{NO}_2(\text{g})$ have been used to produce in situ nitrous acid as the primary source of NO^+ . Starting from the organometallic precursor *fac*- $[\text{MX}_3(\text{CO})_3]^+$, **1** ($\text{M} = {}^{99}\text{Tc}$, Re ; $\text{X} = \text{Cl}$, Br), the formation of mixed dicarbonyl–mononitrosyl complexes was observed in aqueous hydrochloric and hydrobromic acid. Time-dependent analyses of the reactions by means of HATR-IR and ${}^{99}\text{Tc}$ NMR spectroscopy in solution revealed the almost quantitative substitution of one CO ligand by NO^+ and, thus, the formation of complexes with facial arrangement of the three π -acceptor ligands. In the case of technetium, the monomeric complex $(\text{NEt}_4)[\text{TcCl}_3(\text{CO})_2\text{NO}]$ (**3a**) and the dimeric, chloride-bridged, neutral complex $[\text{TcCl}(\mu\text{-Cl})(\text{CO})_2\text{NO}]_2$ (**4a**) were produced. In the case of rhenium, the monomeric species $(\text{NEt}_4)[\text{ReBr}_2\text{X}(\text{CO})_2\text{NO}]$ ($\text{X} = \text{Br}$ (**3b**), NO_3 (**5**)) was solely isolated. The X-ray structure of complexes **4a** and **5** are discussed. The crystallographic analyses revealed the coordination of the NO^+ group trans to the terminal chloride (**4a**) or the bromide (**5**), respectively. Crystal data: complex **4a** ($\text{C}_4\text{Cl}_4\text{N}_2\text{O}_6\text{Tc}_2$), monoclinic, Cc , $a = 18.82(3) \text{ \AA}$, $b = 6.103(6) \text{ \AA}$, $c = 12.15(2) \text{ \AA}$, $\alpha = 90^\circ$, $\beta = 105.8(2)^\circ$, $\gamma = 90^\circ$, $V = 1343(3) \text{ \AA}^3$, $Z = 4$; complex **5** ($\text{C}_{10}\text{H}_{20}\text{N}_3\text{O}_6\text{Br}_2\text{Re}$), orthorhombic, $P2_12_12_1$, $a = 10.2054(5) \text{ \AA}$, $b = 12.5317(7) \text{ \AA}$, $c = 13.9781(7) \text{ \AA}$, $V = 1787.67(16) \text{ \AA}^3$, $Z = 4$. The isolated complexes and their potential *facial* isomers have been further investigated by density functional theory (DFT) calculations. The energy differences of the isomers are relatively small; however, the calculated energies are consistent with the formation of the observed and isolated compounds. The calculated bond lengths and angles of complex **5** are in good agreement with the data determined by X-ray diffraction. Experiments on the no-carrier-added level starting from *fac*- $[\text{}^{99m}\text{Tc}(\text{H}_2\text{O})_3(\text{CO})_3]^+$ revealed the formation of the complex *fac*- $[\text{}^{99m}\text{TcCl}(\text{H}_2\text{O})_2(\text{CO})_2\text{NO}]^+$ in reasonable good yields. This aqueous-based, synthetic approach will enable the future evaluation of this novel, low-valent metal precursor for potential use in radiopharmacy.

Introduction

Complexes of technetium and rhenium in low oxidation states have recently gained considerable attention in the

development of novel, target specific radiopharmaceuticals and cytotoxic agents.^{1,2} In particular, the organometallic aqua ions $[\text{Tc}(\text{H}_2\text{O})_3(\text{CO})_3]^+$ and $[\text{Re}(\text{H}_2\text{O})_3(\text{CO})_3]^+$ not only impelled the basic, aqueous chemistry of these two elements^{3–5}

* To whom correspondence should be addressed. E-mail: roger.schibli@psi.ch. Phone: +41-(0)56-310 2837. Fax: +41-(0)56-310 2849.

† Center for Radiopharmaceutical Science.

‡ Department of Chemistry and Applied Biosciences ETH.

§ Institute of Inorganic Chemistry.

|| Laboratory of Crystallography ETH.

⊥ University of Missouri—Columbia.

(1) Schibli, R.; Schubiger, A. P. *Eur. J. Nucl. Med.* **2002**, *29*, 1529.

(2) Zhang, J. Y.; Vittal, J. J.; Henderson, W.; Wheaton, J. R.; Hall, I. H.; Hor, T. S. A.; Yan, Y. K. *J. Organomet. Chem.* **2002**, *650*, 123.

(3) Aebischer, N.; Schibli, R.; Alberto, R.; Merbach, A. E. *Angew. Chem., Int. Ed.* **2000**, *39*, 254.

but significantly stimulated the development of new organometallic radiopharmaceuticals.^{6–11} This circumstance motivated us to further develop organometallic precursors of Tc and Re for potential use in radiopharmacy.

Apart from employing the tricarbonyl technology for the (radio)labeling of various biomolecules, we are currently investigating the potential of other organometallic synthons for use in radiopharmacy. The linear coordinated NO⁺ ligand is considered to have a lower σ -donor and higher π -acceptor strength than the isolobal CO, resulting in a higher electron acceptor strength as an overall effect. It is well-known that the presence of a NO⁺ strongly affects transition metal centers and their coordination sphere, particularly the substitution lability of ligands in position trans to NO.¹² With respect to organometallic technetium and rhenium complexes for biomedical use, this fact could lead to compounds with different and improved pharmacokinetic properties compared to those labeled with the [M(CO)₃] fragment or simplify the functionalization of biomolecules for radiolabeling with ^{99m}Tc or ¹⁸⁸Re.¹³

Generally halogen–dicarbonyl–nitrosyl synthons of rhenium(I) are formed via substitution reaction starting from [Re(CO)₄X]₂ or [Re(CO)₃X₂]₂ (X = Cl, Br, I) by employing salts of the general formula NOX (X = e.g. BF₄, PF₆) in organic media.^{14–16} The same holds true for low-valent, organometallic technetium nitrosyl compounds.^{17,18} Alternatively Norton and Dolcetti have presented the synthesis of mixed carbonyl–nitrosyl rhenium complexes by purging NO(g) through solutions of [Re(CO)₄X]₂ in benzene or carbon tetrachloride.¹⁹ To our knowledge, the aqueous behavior and particularly the preparation of mixed carbonyl–

nitrosyl complexes of low-valent technetium and rhenium have never been seriously investigated. In view of the development of novel radiopharmaceuticals, it is necessary to search for strategies to prepare such compounds in aqueous media and investigate their chemical behavior and stability under physiological conditions.

In this work, we report for the first time the syntheses and systematic analyses of the formation of mixed dicarbonyl–mononitrosyl complexes of Tc(I)/Re(I) in aqueous hydrochloric or hydrobromic acid starting from (NEt₄)₂[MX₃(CO)₃] (M = ⁹⁹Tc, X = Cl (**1a**); M = Re, X = Br (**1b**)) by means of HATR-IR and ⁹⁹Tc NMR experiments. Density functional calculations of the isolated and characterized complexes and their potential structural isomers are reported. In addition the radiosynthesis of *fac*-[^{99m}TcCl(H₂O)₂(CO)₂-NO]²⁺ on the no-carrier-added level starting from *fac*-[^{99m}Tc(H₂O)₃(CO)₃]⁺ in physiological saline is described.

Experimental Section

All chemicals were purchased from Aldrich Chemical Co., Sigma, or Fluka, Buchs, Switzerland. The chemicals and solvents were of reagent grade and used without further purification. Na-[^{99m}TcO₄] was eluted from a ⁹⁹Mo/^{99m}Tc generator (Mallinckrodt, Petten, The Netherlands) using 0.9% saline. (NEt₄)₂[⁹⁹TcCl₃(CO)₃] (**1a**), (NEt₄)₂[ReBr₃(CO)₃] (**1b**), and [^{99m}Tc(H₂O)₃(CO)₃]⁺ were synthesized according to previously published procedures.^{20–22} Nuclear magnetic resonance spectra were recorded on a 300 MHz Varian Gemini 2000 spectrometer. The ¹H and ⁹⁹Tc chemical shifts are reported relative to residual solvent protons or TcO₄[−] (0 ppm) as a reference. IR spectra were recorded on a Perkin-Elmer FT-IR 16PC using KBr pellets or a ZnSe HATR device for IR spectra recorded in aqueous solution. HPLC analyses were performed on a Merck-Hitachi L-7000 system equipped with an L-7400 tunable absorption detector and a Berthold LB 506 B radiometric detector. HPLC solvents consisted of aqueous 0.05 M TEAP (triethylammonium phosphate) buffer, pH = 2.25 (solvent A), and methanol (solvent B). For the radiochemical analyses a Macherey-Nagel C-18 reversed phase column (10 μ m, 150 \times 4.1 mm) was used. The HPLC system started with 100% of A from 0 to 3 min. The eluent switched at 3 min to 75% A and 25% B and at 9 min to 66% A and 34% B followed by a linear gradient 66% A/34% B to 100% B from 9 to 20 min. The thin-layer chromatography (TLC) system was performed using glass-backed silica gel plates (Merck 60F₂₅₄, mobile phase of 99% methanol and 1% concentrated HCl). The plates were scanned with a Burkard RAYTEST RITA-3200 radioanalyzer. Radioactive samples were counted in a Canberra Packard COBRA II auto γ well counter.

Caution! All operations with radioactive material (⁹⁹Tc and ^{99m}Tc) have been carried out in specially equipped laboratories to avoid contamination or ingestion.

Aqueous Synthesis of Complexes NEt₄[TcCl₃(CO)₂NO] (3a) and [TcCl(μ -Cl)(CO)₂NO]₂ (4a). Method A. Precursor **1a** (55 mg, 0.1 mmol) was dissolved in 2 mL of a mixture of H₂O/1 M HCl/concentrated H₂SO₄ (2/1/0.1 v/v). NaNO₂ (54 mg, 1.2 mmol) was added and the reaction solution stirred at 60 °C for 12 h. The volume

- (4) Salignac, B.; Grundler, P. V.; Cayemites, S.; Frey, U.; Scopelliti, R.; Merbach, A. E.; Hedinger, R.; Hegetschweiler, K.; Alberto, R.; Prinz, U.; Raabe, G.; Kolle, U.; Hall, S. *Inorg. Chem.* **2003**, *42*, 3516.
- (5) Egli, A.; Hegetschweiler, K.; Alberto, R.; Abram, U.; Schibli, R.; Hedinger, R.; Gramlich, V.; Kissner, R.; Schubiger, P. A. *Organometallics* **1997**, *16*, 1833.
- (6) La Bella, R.; Garcia-Garayoa, E.; Bahler, M.; Blauenstein, P.; Schibli, R.; Conrath, P.; Tourwe, D.; Schubiger, P. A. *Bioconjugate Chem.* **2002**, *13*, 599.
- (7) Langer, M.; La Bella, R.; Garcia-Garayoa, E.; Beck-Sickinger, A. G. *Bioconjugate Chem.* **2001**, *12*, 1028.
- (8) Garcia-Garayoa, E.; Blauenstein, P.; Bruehlmeier, M.; Blanc, A.; Iterbeke, K.; Conrath, P.; Tourwe, D.; Schubiger, P. A. *J. Nucl. Med.* **2002**, *43*, 374.
- (9) Hoepping, A.; Reisgys, M.; Brust, P.; Seifert, S.; Spies, H.; Alberto, R.; Johannsen, B. *J. Med. Chem.* **1998**, *41*, 4429.
- (10) Egli, A.; Alberto, R.; Tannahill, L.; Schibli, R.; Abram, U.; Schaffland, A.; Waibel, R.; Tourwe, D.; Jeannin, L.; Iterbeke, K.; Schubiger, P. A. *J. Nucl. Med.* **1999**, *40*, 1913.
- (11) Alberto, R.; Schibli, R.; Schubiger, P. A.; Abram, U.; Pietzsch, H. J.; Johannsen, B. *J. Am. Chem. Soc.* **1999**, *121*, 6076.
- (12) Bezerra, C. W. B.; da Silva, S. C.; Gambardella, M. T. P.; Santos, R. H. A.; Plicas, L. M. A.; Tfouni, E.; Franco, D. W. *Inorg. Chem.* **1999**, *38*, 5660.
- (13) Schibli, R.; La Bella, R.; Alberto, R.; Garcia-Garayoa, E.; Ortner, K.; Abram, U.; Schubiger, P. A. *Bioconjugate Chem.* **2000**, *11*, 345.
- (14) Veghini, D.; Nefedov, S. E.; Schmalle, H.; Berke, H. *J. Organomet. Chem.* **1996**, *526*, 117.
- (15) Uguagliati, P.; Zingales, F.; Trovati, A.; Cariati, F. *Inorg. Chem.* **1971**, *10*, 507.
- (16) Rattat, D.; Schubiger, P. A.; Berke, H. G.; Schmalle, H.; Alberto, R. *Cancer Biother. Radiopharm.* **2001**, *16*, 339.
- (17) Linder, K. E.; Davison, A.; Deean, J. C.; Costello, C.; Maleknia, S. *Inorg. Chem.* **1986**, *25*, 2085.
- (18) Knight Castro, H. H.; Meetsma, A.; Teuben, J. H.; Vaalburg, W.; Panek, K.; Ensing, G. *J. Organomet. Chem.* **1991**, *410*, 63.
- (19) Norton, J. R.; Dolcetti, G. L. *Inorg. Chem.* **1973**, *12*, 485.

- (20) Alberto, R.; Schibli, R.; Egli, A.; Schubiger, P. A.; Herrmann, W. A.; Artus, G.; Abram, U.; Kaden, T. A. *J. Organomet. Chem.* **1995**, *493*, 119.
- (21) Alberto, R.; Ortner, K.; Wheatley, N.; Schibli, R.; Schubiger, P. A. *J. Am. Chem. Soc.* **2001**, *123*, 3135.
- (22) Alberto, R.; Schibli, R.; Schubiger, P. A.; Abram, U.; Kaden, T. A. *Polyhedron* **1996**, *15*, 1079.

of the reaction was reduced to 0.5 mL. After the reaction was cooled to 0 °C, the dark yellow products were extracted twice with 5 mL of ethyl acetate. The organic layers were dried over Na₂SO₄, and the solvent was evaporated. Composition based on ⁹⁹Tc NMR: 55% **3a** and 45% **4a**. Yield: 35 mg (71% with respect to Tc).

Method B. Precursor **1a** (50 mg, 0.09 mmol) was dissolved in 2 mL of 1 M HCl. NOHSO₄ (48 mg, 1.2 mmol) was added and the reaction stirred at 60 °C for 12 h. After reduction of the volume to 0.5 mL and cooling, the dark yellow products were extracted twice with 5 mL of ethyl acetate. The organic layers were dried over Na₂SO₄, and the solvent was evaporated. Composition based on ⁹⁹Tc NMR: 43% **3a** and 57% **4a**. Yield: 28 mg (59% with respect to Tc). Analytical data for **3a**: ⁹⁹Tc NMR (CDCl₃) –460 ppm; IR (cm⁻¹) 2101 (CO), 2039 (CO), 1775 (NO). Analytical data for **4a**: ⁹⁹Tc NMR (CDCl₃) –389 ppm; IR (cm⁻¹) 2116 (CO), 2062 (CO), 1822 (NO).

Aqueous Synthesis of Complex NEt₄[ReBr₃(CO)₂NO] (3b).
Method A. Precursor **1b** (75 mg, 0.09 mmol) was dissolved in 2 mL of a mixture of H₂O/1 M HBr/concentrated H₂SO₄ (2/1/0.1 v/v). A total of 4 equiv of NaNO₂ was added and the reaction solution stirred at 60 °C for 2 h. The volume of the reaction was reduced to 0.5 mL. After cooling, the product partially precipitated from the solution and was filtered. After further reduction of the mother liquor, more of the product could be isolated via extraction twice with 5 mL of ethyl acetate. The organic layers were dried over Na₂SO₄, and the solvent was evaporated. Yield: 65 mg (75%).

Method B. Precursor **1b** (75 mg, 0.09 mmol) was dissolved in 1 M HBr. A total of 4 equiv of NOHSO₄ was added and the reaction stirred at 60 °C for 2 h. After cooling, the dark yellow products were extracted twice with 5 mL of ethyl acetate. The organic layers were dried over Na₂SO₄, and the solvent was evaporated. Yield: 55 mg (63%). Analytical data for **3b**: IR (cm⁻¹) 2090 (CO), 2016 (CO), 1775 (NO). Anal. Calcd for C₁₀H₂₀N₂O₃Br₃Re: C, 18.70; H, 3.14; N, 4.36. Found: C, 18.53; H, 3.29; N, 4.22. EIMS: *m/z* 512 [M⁺ – NEt₄].

Synthesis of Complex NEt₄[ReBr₂(NO₃)(CO)₂NO] (5). The precursor **1b** (79 mg, 0.11 mmol) was dissolved in 2 mL of 1 M HBr. NO₂(g) was purged through the solution at 50 °C for 1 h. The reaction was kept at 70 °C for an additional 2 h. The color of the reaction solution changed gradually from colorless to yellow. After cooling, the reaction solution was neutralized with Na₂CO₃, the solution concentrated to 0.5 mL, and the dark yellow product extracted three times with 5 mL of thf. The organic layers were dried over Na₂SO₄, and the solvent was evaporated in a vacuum. Crystals of X-ray quality could be grown by slow diffusion of hexane into a solution of the product in thf. Yield: 48 mg, 52%. Analytical data for **5**: IR (cm⁻¹) 2093 (CO), 2020 (CO), 1780 (NO), 1273 (NO₃). Anal. Calcd for C₁₀H₂₀N₃O₆Br₂Re: C, 19.23; H, 3.23; N, 6.73. Found: C, 19.34; H, 3.17; N, 6.52. EIMS: *m/z* 494 [M⁺ – NEt₄].

Synthesis of Complexes NEt₄[TcCl₃(CO)₂NO] (3a) in Organic Media. The precursor **1a** (39 mg, 0.07 mmol) was suspended in 10 mL of freshly dried thf. A 40 mg amount of NOBF₄ (0.35 mmol) was added and the reaction solution stirred at room temperature for 2 h. Consumption of the starting material **1a** was monitored via ⁹⁹Tc NMR. After removal of the solvent, the dark yellow residue was recrystallized from chloroform. Yield: 22 mg, 75%. Analytical data: ⁹⁹Tc NMR (CDCl₃) –460 ppm; IR (cm⁻¹) 2101 (CO), 2039 (CO), 1775 (NO).

Synthesis of Complex [^{99m}TcCl(H₂O)₂(CO)₂NO]²⁺. To 500 μL of a freshly prepared solution of [^{99m}Tc(H₂O)₃(CO)₃]⁺ (pH = 7) was added 50 μL of concentrated HCl. This solution was injected into a sealed 10 mL vial containing 15 mg of solid NOHSO₄. The

Table 1. Crystal Data and Details of Data Collection for Complexes **4a** and **5**

	4a	5
formula	C ₄ Cl ₄ N ₂ O ₆ Tc ₂	C ₁₀ H ₂₀ N ₃ O ₆ Br ₂ Re
fw	509.86	624.29
cryst size (mm)	0.09 × 0.05 × 0.03	0.1 × 0.25 × 0.25
space group	Cc	P2 ₁ 2 ₁ 2 ₁
<i>a</i> (Å)	18.82(3)	10.2054(5)
<i>b</i> (Å)	6.103(6)	12.5317(7)
<i>c</i> (Å)	12.151(16)	13.9781(7)
β (deg)	105.80(17)	90
<i>V</i> (Å ³)	1343(3)	1787.67(16)
<i>Z</i>	4	4
temp (K)	293(2)	173(2)
<i>D_c</i> (g/cm ³)	2.521	2.320
μ (mm ⁻¹)	24.267	11.295
<i>F</i> (000)	960	1176
radiatn	Cu Kα	Mo Kα
wavelength (Å)	1.541 78	0.710 70
θ range (deg)	4.88–49.92	2.18–27.15
no. of collcd reflns	707	11 038
no. of obsd reflns	691	3579
GOF	1.088	0.995
wR2/R1 ^a (%)	8.60/3.55	5.05/2.67

$$^a \text{wR2} = \{[\sum w(F_o - F_c)^2]/\sum wF_o^2\}^{1/2} \text{ and } \text{R1} = \sum |F_o| - |F_c|/\sum F_o.$$

formation of colorless NO(g) and brown NO₂(g) was instantaneously observed. The solution was kept at 100 °C for 10 min before cooling on ice. The solution was neutralized with a 1:1 mixture of phosphate buffer and 10 N NaOH (final pH = 6.5). Yield: >85% (based on TLC).

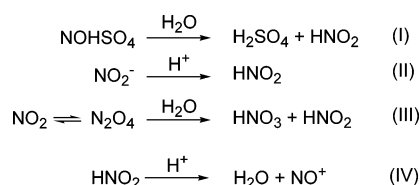
X-ray Data Collection and Processing. Details of the data collection, structure solution, and refinement for complexes **4a** and **5** are presented in Table 1. The intensities for the X-ray determination were collected on a Picker-Stoe (**4a**) and a Siemens SMART CCD (**5**) system using Cu Kα (**4a**) and Mo Kα (**5**) radiation, respectively. The ω scan mode was applied in both cases. The structures were solved by heavy-atom Patterson synthesis using SHELXS-86, and the refinements were performed with SHELXL-93 (**4a**) or with the NRCVAX system (**5**).^{23–25} For compound **5** data were corrected for decay and absorption using the program SADABS based on the method of Blessing.²⁶ Crystal data and more details of the collection and refinements are contained in Table 1. Atomic coordinates and their equivalent isotropic displacement coefficients are included in the Supporting Information.

Computational Details

Density functional theory (DFT) calculations were performed at the generalized gradient approximation (GGA) level of theory. All calculations were carried out with the software package ADF2003.01.^{27,28} The BP86 exchange-correlation energy functional^{29,30} was used, as this functional gives excellent structural agreement with experiment in the case of other low-valent Tc and Re complexes. The “TZP” basis set of the ADF package was used. This basis set is triple-ζ with one polarization function in the valence

- Gabe, E. J.; Le Page, Y.; Charland, J.-P.; Lee, F. L.; White, P. S. J. *Appl. Crystallogr.* **1989**, *22*, 384.
- Sheldrick, G. M. *SHELXS86 -A program for the resolution of X-ray structures*; University of Göttingen: Göttingen, Germany, 1986.
- Sheldrick, G. M. *SHELXL-93*; University of Göttingen: Göttingen, Germany, 1993.
- Blessing, *Acta Crystallogr.* **1995**, *A51*, 33.
- Vera, D. R.; Wallace, A. M.; Hoh, C. K. *Nucl. Med. Biol.* **2001**, *28*, 493.
- Guerra, C. F.; Snijders, J. G.; te Velde, G.; Baerends, E. J. *Theor. Chem. Acc.* **1998**, *99*, 391.
- Becke, A. D. *Phys. Rev. A* **1988**, *38*, 3098.
- Perdew, J. P.; Yue, W. *Phys. Rev. B* **1986**, *33*, 8800.

Scheme 1



region and double- ζ in the core region. The frozen core approximation was applied (for electrons up to the 1s shell for C, N, O; up to 2p for Cl; 3d for Tc, Br; 4d for Re) and a spin-restricted formalism. Spin-unrestricted calculations and calculations with larger basis sets (“TZ2P”, “QZ4P”) were performed on compounds **4a** and **5** to ensure that our chosen level of theory is appropriate. The ZORA approach^{31–33} was used to incorporate scalar relativistic effects.

Results and Discussion

Synthesis and Characterization of Dicarbonyl–Mononitrosyl Complexes of Technetium(I) and Rhenium(I). An aqueous readily accessible source of NO^+ in acidic, oxygen-free media is nitrous acid, HNO_2 . For this work we employed NO_2^- , NOHSO_4 , or $\text{NO}_2(\text{g})$, which produce HNO_2 e.g. during dissociation or disproportionation according to Scheme 1.

All reactions on the macroscopic scale started from *fac*- $[\text{MX}_3(\text{CO})_3]^{2-}$ ($\text{M} = {}^{99}\text{Tc}$, $\text{X} = \text{Cl}$ (**1a**); $\text{M} = \text{Re}$, $\text{X} = \text{Br}$ (**1b**)), which forms readily *fac*- $[\text{M}(\text{H}_2\text{O})_3(\text{CO})_3]^+$ ($\text{M} = {}^{99}\text{Tc}$ (**2a**), Re (**2b**)) in water.²⁰ The precursors **1a,b** have been dissolved in 1 M HX ($\text{X} = \text{Cl}$, Br), and the solutions were purged with nitrogen. NaNO_2 or NOHSO_4 has been added under an atmosphere of nitrogen. The formation of colorless $\text{NO}(\text{g})$ as well as traces of brown $\text{NO}_2(\text{g})$ was instantaneously observed. In the case of ${}^{99}\text{Tc}$ the color of the reaction solution changed from colorless to green-yellow after heating. The reaction was followed by radio-TLC (99/1 methanol/concentrated HCl). Analyses of the reaction solution revealed beside ${}^{99m}\text{TcO}_2$ (at origin; <10%) traces of TcO_4^- ($R_f = 0.8$; <4%) and additionally a broad signal with an R_f value of 0.15. After completion of the reaction, the solution was concentrated and cooled to 0 °C (Scheme 2). Most of the product could be extracted with ethyl acetate. After removal of the organic solvent, the product mixture gave a dark yellow glassy residue. The IR spectrum of the isolated product revealed the typical facial “ $\text{M}(\text{CO})_2\text{NO}$ ” pattern. The broadening of the intense signals at 2118 cm^{-1} ($\nu(\text{CO})$), 2062 cm^{-1} ($\nu(\text{CO})$), and 1820 cm^{-1} ($\nu(\text{NO})$) (spectra recorded in KBr) gave rise to the assumption that more than one species was present in the final extract. This could be corroborated in the ${}^{99}\text{Tc}$ NMR spectrum (recorded in CDCl_3), with two broad signals at –389 ppm (approximately 40% abundance) and –460 ppm (approximately 60% abundance). The peak at –460 ppm could be assigned to the complex **3a**, which has been synthesized as a reference classically, starting from **2a** in thf using NOBF_4 (see Experimental Section). The second species, which turned out to be the neutral, dimeric

compound $[\text{TcCl}(\mu\text{-Cl})(\text{CO})_2\text{NO}]_2$ (**4a**), partially crystallized as dark yellow-orange needles from an ethyl acetate/hexane mixture. The IR spectrum of **4a** showed sharp and intense absorptions of $\nu(\text{CO})$ at 2116 and 2062 cm^{-1} and of $\nu(\text{NO})$ at 1822 cm^{-1} , whereas complex **3a** revealed red-shifted intense signals for $\nu(\text{CO})$ at 2101 and 2039 cm^{-1} and of $\nu(\text{NO})$ at 1775 cm^{-1} . The corresponding rhenium complex reported in the literature revealed IR absorptions at 2083, 2006, and 1751 cm^{-1} .³⁴ The ${}^{99}\text{Tc}$ NMR of the recrystallized product **4a**, recorded in CDCl_3 , showed the resonance at –389 ppm. Attempts to quantitatively separate the two products via column chromatography failed. The compounds **3a** and **4a** were soluble in most organic solvents but insoluble in aromatic hydrocarbons.

In contrast to technetium, we observed for rhenium the formation of a single product after addition of NO_2^- or NOHSO_4 . Furthermore, the reaction was completed already after 2 h at 60 °C as evident from TLC and IR analyses. The yellow, monomeric product partially precipitated as crystalline clusters directly from a concentrated reaction solution at room temperature and/or was extracted with ethyl acetate. The IR spectrum revealed very strong absorptions at 2090 cm^{-1} , 2016 cm^{-1} ($\nu(\text{CO})$), and 1775 cm^{-1} ($\nu(\text{NO})$). The presence of the monomeric, monoanionic complex **3b** was evident from elemental and mass spectrometric analyses as well as X-ray structure determination (X-ray data included in the Supporting Information).

Reactions with gaseous nitric dioxide were performed by purging an aqueous solution of **1b** in 1 M HBr for 1 h at 50 °C with NO_2 . The faintly yellow reaction solution was heated for 2 h at 70 °C until the color changed to dark yellow (Scheme 3). The reaction solution was neutralized with Na_2CO_3 and the product extracted with thf from the large excess of $\text{NaNO}_3/\text{NaNO}_2$. The crude product revealed CO and NO stretch bands at 2093, 2020, and 1780 cm^{-1} (with additional N–O absorption at 1273 cm^{-1} of NO_3^-) of the product **5**. Crystals of complex **5** suitable for X-ray structure analyses could be grown by slow diffusion of hexane into a thf solution of the complex. The coordination of a nitrate instead of a third bromide can be explained by the large excess of NO_3^- in the reaction solution after neutralization.

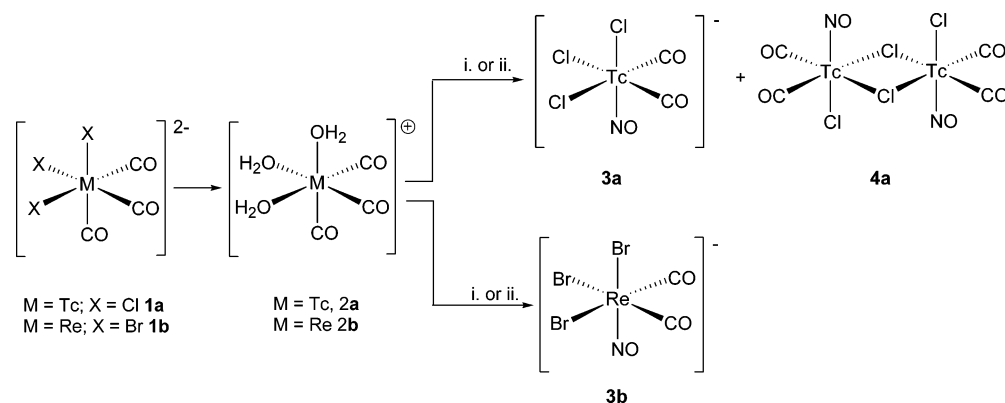
HATR-IR Experiments and ${}^{99}\text{Tc}$ NMR. The reactions with **1a,b** in the presence of NaNO_2 and HX ($\text{X} = \text{Cl}$, Br) have been monitored by means of ${}^{99}\text{Tc}$ NMR and HATR-IR spectroscopy in aqueous solutions. Figure 1 depicts the time-dependent IR spectra in the region between 2200 and 1700 cm^{-1} of the reaction with **1b** in aqueous hydrobromic acid. Spectrum A represents the solvated starting material $[\text{Re}(\text{H}_2\text{O})_3(\text{CO})_3]^+$ (**2b**) with the characteristic $\text{M}(\text{CO})_3$ pattern (2032, 1910 cm^{-1}).²⁰ After 1 h at 60 °C three new absorption bands appeared at 2114 and 2038 cm^{-1} (with a shoulder at approximately 2040 cm^{-1}) and 1804 cm^{-1} , which evidenced the presence of considerable amounts of a “ $\text{M}(\text{CO})_2\text{NO}$ ” species (Figure 1B). After 2 h the starting material was almost completely consumed and intense absorptions

(31) van Lenthe, E.; Baerends, E. J.; Snijders, J. G. *J. Chem. Phys.* **1994**, *101*, 9783.

(32) van Lenthe, E.; Baerends, E. J.; Snijders, J. G. *J. Chem. Phys.* **1993**, *99*, 4597.

(33) van Lenthe, E.; Ehlers, A.; Baerends, E. J. *J. Chem. Phys.* **1999**, *110*, 8943.

(34) Hubbard, J. L.; Kimball, K. L.; Burns, R. M.; Sum, V. *Inorg. Chem.* **1992**, *31*, 424.

Scheme 2^a

^a Key: (i) 4 equiv of NOHSO₄, 1 M HX (X = Cl, Br), 60 °C; (ii) 4 equiv of NaNO₂, 1 M HX (X = Cl, Br), 60 °C.

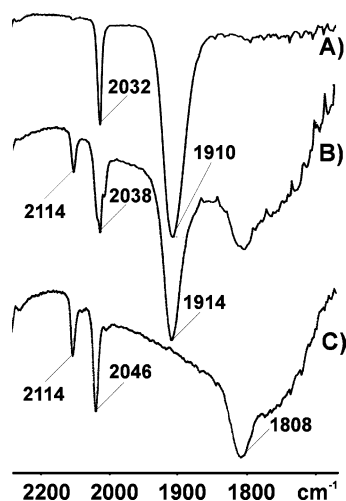
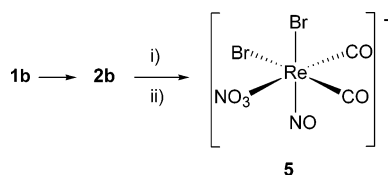


Figure 1. Time-dependent IR spectra of the reaction in the presence of NO₂⁻ or NOHSO₄ in aqueous hydrobromic acid: (A) [Re(H₂O)₃(CO)₃]⁺; (B) reaction after 1 h at 60 °C; (C) reaction after 2 h at 60 °C.

Scheme 3^a

^a Key: (i) 1 M HBr, NO₂(g), 2 h, 70 °C; (ii) Na₂CO₃.

at 2114, 2046, and 1808 cm⁻¹ could be detected (Figure 1C). Retrospective analyses of a 10⁻² M solution of complex **3b** in 1 M trifluoromethanesulfonic acid before and after precipitation of 2 equiv of bromides with AgCF₃SO₃ revealed signals at 2116, 2040, and 1796 cm⁻¹. (The IR spectrum of complex [Re(H₂O)₃(CO)₂NO]²⁺ recorded under the same conditions revealed signals at 2121, 2054, and 1824 cm⁻¹.) Thus, it can be concluded that spectrum C in Figure 1 represent the species with the composition [ReBr(H₂O)₂(CO)₂NO]⁺.

⁹⁹Tc NMR experiments were performed in 1 M HCl (1/1 mixture of H₂O/D₂O). Samples of 0.5 mL were taken and recorded every 3 h. Figure 2A depicts the ⁹⁹Tc NMR spectrum of starting material **2a** with a resonance at -865 ppm. This is only slightly low-field shifted compared to the resonance recorded in pure D₂O (-873 ppm).²² After 3 h,

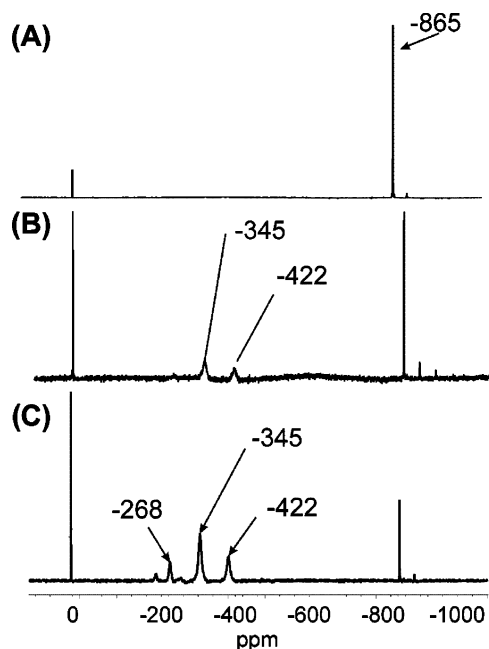


Figure 2. Time-dependent ⁹⁹Tc NMR spectra of the reaction in aqueous hydrochloric acid using NO₂⁻ or NOHSO₄: (A) [Tc(H₂O)₃(CO)₃]⁺; (B) reaction after 3 h at 60 °C; (C) reaction after 12 h at 60 °C.

the intensity of the signal at -865 ppm decreased (57%), while two broad peaks at -422 ppm (15%) and -345 ppm (25%) appeared (Figure 2B). After 12 h the starting material had essentially disappeared and the signals at -422 ppm (25%) and -345 ppm (48%) dominated the spectrum (Figure 2C). In addition a peak at -268 ppm could be observed (intensity 12%). On the basis of the reference spectrum of complex **3a** (and the data observed with **4a**) in 1 M HCl, we can assign the signals of the reaction solution as follows: The signal at -422 ppm represents the neutral, monosolvated species [TcCl₂(H₂O)(CO)₂NO]⁰. The major signal at -345 ppm arises from the cationic, bisolvated complex [TcCl(H₂O)₂(CO)₂NO]⁺. The signal at -268 ppm originates from the tris(aqua) complex [Tc(H₂O)₃(CO)₂NO]²⁺, present only in low concentration.

Particularly from the ⁹⁹Tc NMR experiments it can be concluded that in acidic aqueous media the mono-, bis-, and tris(aqua) species of **3a,b** are present in solution; however the bis(aqua) complex is dominant (Scheme 4). This holds

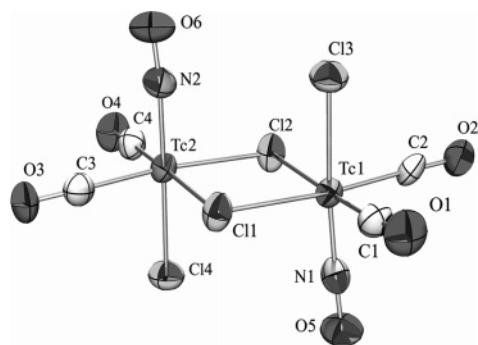
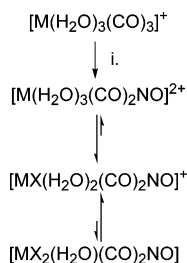


Figure 3. ORTEP diagram of compound **4a**. Atoms are drawn on the 50% probability level.

Scheme 4^a



^a Key: (i) NO⁺, X⁻ (X = Cl, Br).

true also for the reaction on the no-carrier-added level with ^{99m}Tc (vide infra). This is in contrast to the situation of **1a,b** in aqueous media, where only the tris(aqua) species **2a,b** are present.²⁰ This fact can readily be explained by the strong π -acceptor strength and/or the additional positive charge introduced via NO⁺, which favors the (re-)coordination of at least one halide. At increasing halide concentration the equilibrium in solution can be shifted toward [MX₂(H₂O)(CO)₂NO]⁰ and [MX₃(CO)₂NO]⁻, respectively. Later one precipitates eventually from the reaction solution as mentioned earlier. Thus, only when dissolved in very weakly coordinating, organic solvents (e.g. CHCl₃ or CH₂Cl₂) spectra of the nonsolvated species **3a,b** and **4a** can be recorded. At present, we do not have a conclusive explanation for the absence of a dimeric complex in the case of rhenium since the reaction condition and workup procedure were identical, except for the nature of the halides.

From our previous investigations of the exchange rate of metal-coordinated CO ligand in aqueous media,³ it is reasonable to assume that the exchange of a CO ligand by a NO⁺ takes place via an intermediate “[MNO(CO)₃]²⁺” species. The loss of the CO ligand is a consequence of the stronger trans effect of the coordinated NO⁺. Density functional calculations performed on [MNO(H₂O)₂(CO)₃]²⁺ further support this assumption. The calculations predicted a significant elongation of the M–CO bond (2.12 Å in the case of Tc and 2.11 Å for Re) trans to the NO ligand versus 1.99 Å (Tc) and 1.98 Å (Re) trans to the coordinated water molecules.

Crystal Structure of Complex 4a. Prismatic crystals of X-ray quality were obtained by slow diffusion of hexane into a solution of **4a** in CH₂Cl₂ at room temperature. The ORTEP diagram of the dimeric complex **4a** is shown in Figure 3. Bond lengths and angles are given in Table 2. The unit cell

Table 2. Selected Bond Lengths (Å) and Angles (deg) from the X-ray Structure of **4a**

Tc1–N1	1.749(14)	Tc2–C3	1.94(2)
Tc1–C1	1.95(2)	Tc2–C4	1.96(2)
Tc1–C2	1.96(2)	Tc2–Cl4	2.380(5)
Tc1–Cl3	2.375(5)	Tc2–Cl1	2.468(5)
Tc1–Cl2	2.455(5)	Tc2–Cl2	2.471(6)
Tc1–Cl1	2.471(6)	O1–C1	1.13(2)
N1–O5	1.16(2)	O3–C3	1.15(2)
O4–C4	1.10(2)	N2–O6	1.13(2)
Tc2–N2	1.794(14)	O2–C2	1.15(2)
Cl3–Tc1–Cl2	89.3(2)	Cl1–Tc2–Cl2	83.18(14)
C1–Tc1–C2	90.2(5)	Cl4–Tc2–Cl2	88.79(15)
O5–N1–Tc1	177.4(8)	C4–Tc2–Cl2	92.2(3)
O1–C1–Tc1	175.5(10)	C3–Tc2–Cl2	173.7(4)
N1–Tc1–C2	90.3(4)	N2–Tc2–Cl2	91.7(3)
N1–Tc1–Cl1	91.0(4)	Cl4–Tc2–Cl1	89.34(12)
O2–C2–Tc1	178.0(9)	C3–Tc2–Cl1	92.0(4)
N1–Tc1–Cl3	175.4(3)	N2–Tc2–Cl1	92.5(3)
Cl2–Tc1–Cl1	83.51(14)	C3–Tc2–Cl4	87.1(3)
Cl3–Tc1–Cl1	89.36(15)	N2–Tc2–Cl4	178.1(3)
C2–Tc1–Cl3	86.7(3)	C3–Tc2–C4	92.2(5)
C2–Tc1–Cl1	174.5(3)	N2–Tc2–C4	93.2(4)
N1–Tc1–Cl1	93.9(3)	O4–C4–Tc2	177.1(9)
C1–Tc1–Cl2	174.0(3)	N2–Tc2–C3	92.6(4)
C2–Tc1–Cl2	92.7(3)	O3–C3–Tc2	172.3(10)
N1–Tc1–Cl2	94.3(3)	O6–N2–Tc2	174.3(9)
C1–Tc1–Cl3	85.7(3)	C4–Tc2–Cl1	172.7(3)
Tc1–Cl2–Tc2	96.80(14)	Tc2–Cl1–Tc1	96.50(14)

of **4a** contains four binuclear technetium complexes. Complex **4a** is centrosymmetric, and the packing diagram view along *b* strongly suggested *C2/c* as the appropriate symmetry. However, the projection along the crystallographic direction *a* unveiled the packing evidently requires that the molecular centers are shifted in the *b* direction away from the *c* glide planes thus making a crystallographic arrangement with the molecules in special centrosymmetric positions impossible. Furthermore, a refinement in *C2/c*, although possible, implied the suspect feature of invariably strong elongations of all ellipsoids, particularly including the heavy atoms, along crystallographic direction *b*. Therefore, the space group *Cc* has been selected for the refinement. Although the X-ray structure of complex **4a** is underdetermined, interesting structural features of this mixed carbonyl–nitrosyl complexes could be still observed. The technetium centers are connected by chloride bridges giving rise to an almost planar arrangement (Cl1–Tc1–Cl2–Tc2 = 1.04(2)°). The Tc–Cl distances range from 2.455(5) Å (Tc1–Cl2) to 2.471(6) Å (Tc2–Cl2). In contrast, the bond lengths of the terminal chlorides are approximately 0.1 Å shorter (Tc1–Cl3 = 2.375(5) Å; Tc2–Cl4 = 2.380(5) Å) due to the strong π -acceptor ligand NO⁺ in the axial, trans position. The Tc–N distances (Tc1–N1 = 1.749(14) Å; Tc2–N2 = 1.794(14) Å) are significantly shorter than the Tc–C bonds (mean 1.95(2) Å). The Tc–N–O angles deviate only slightly from linearity (O5–N1–Tc1 = 177.2(13)°; O6–N2–Tc2 = 174.5(14)°). The same holds true for three of the T–C–O angles (174.5(14)–178.0(14)°) whereas Tc2–C3–O3 (172.0(15)°) is slightly bended. The essentially linear coordination of the NO⁺ and CO is appropriate for the electronic configuration, where the ligands act as two electron donors.

Crystal Structure of Complex 5. The ORTEP diagram of the complex anion of **5** is shown in Figure 4. Selected

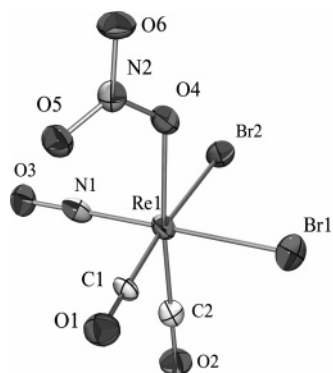


Figure 4. ORTEP diagram of the complex anion of compound **5**. Atoms are drawn on the 30% probability level.

Table 3. Selected Bond Lengths (Å) and Angles (deg) from X-ray Structure Data and from DFT Optimization of **5**

param	X-ray data	DFT data
Re1–Br1	2.5634(7)	2.598
Re1–Br2	2.5705(7)	2.636
Re1–O4	2.142(4)	2.155
Re1–N1	1.838(5)	1.800
Re1–C1	1.902(5)	1.953
Re1–C2	1.939(7)	1.966
O2–C2	1.150(8)	1.159
O3–N1	1.168(7)	1.183
O6–N2	1.233(7)	1.244
O4–N2	1.285(6)	1.253
Br1–Re1–Br2	88.293(22)	89.53
Br1–Re1–N1	178.65(15)	177.14
Br1–Re1–C1	85.74(17)	83.48
Br1–Re1–C2	90.46(17)	93.11
Br2–Re1–O4	83.99(11)	84.25
O4–Re1–C2	173.83(20)	172.06
N1–Re1–C1	93.00(22)	93.85
N1–Re1–C2	90.04(24)	92.01
C1–Re1–C2	90.24(24)	91.70
Re1–O4–N2	123.2(3)	120.12

bond lengths and angles are given in Table 3. The two CO and the NO⁺ ligand are facially arranged around the pseudooctahedral coordinated metal center. The Re–C bonds (Re1–C1 = 1.902(5) Å; Re1–C2 = 1.939(7) Å) are slightly longer than the rhenium nitrosyl distance (Re1–N1 = 1.838(5) Å). The nitrate molecule (Re1–O4 = 2.142(4) Å) is monodentately coordinated trans to a CO ligand, whereas the NO molecule is located trans to a bromide (Re1–Br2 = 2.5705(7) Å). The CO and NO ligands are linear coordinated (Re1–N1–O3 = 177.9(4)°; Re1–C1–O1 = 178.9(5)°; Re1–C2–O2 = 178.7(5)°). The bend coordinated NO₃[−] molecule (Re1–O4–N2 = 123.2(3)°) points away from the bulky bromides and is positioned between the CO and the NO ligand (torsion angle C1–Re1–O4–N2 = 39.1°).

Density Functional Calculations. As a first step, geometry optimizations of complexes **4a** and **5** were performed to evaluate the quality of our computational approach. The optimized bond lengths and angles of both species match generally well those from the X-ray structure analyses (see also Supporting Information). For the monomeric rhenium complex **5** the metal–nitrosyl bond was calculated to be 1.80 Å and has been determined experimentally as 1.84 Å. The average calculated M–CO bond length was found to be 1.96 Å whereas the experimentally determined values were 1.90

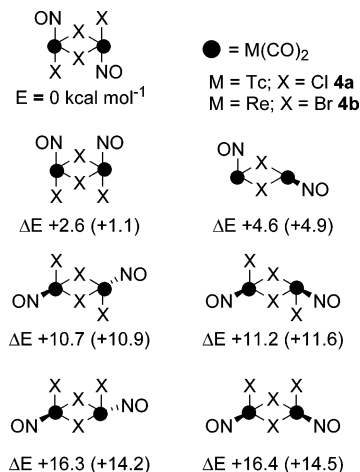
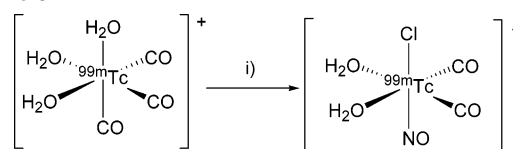


Figure 5. Relative differences in binding energies of structural isomers of complexes **4a,b** (values of **4b** in parentheses).

Scheme 5^a



^a Key: (i) NOHSO₄, 1 M HCl, 10 min, 100 °C.

and 1.94 Å. The quality of the X-ray structure of complex **4a** did not allow a quantitative comparison with the data obtained via DFT calculations.

In a second step, we performed geometry optimizations of a number of alternative isomers of **4a** and **5**. The respective energies for the isomers of complex **4a** were between 2.6 and 16.4 kcal mol^{−1} higher, indicating that the chemically isolated species is indeed the most stable (Figure 5). Similar results were found for the corresponding complex [ReBr(μ-Br)(CO)₂NO]₂ (data in the Supporting Information). In the case of complex **5** it was found that the potential isomer, where the NO ligand is trans to nitrate, is 2.3 kcal mol^{−1} less stable than the actually isolated species.

Reaction on the No-Carrier-Added Level with Technetium-99m. For the reactions on the no-carrier-added level the clinically most widely used diagnostic isotope technetium-99m (γ ; $T_{1/2} = 6$ h) was used. A freshly prepared solution²¹ of [^{99m}Tc(H₂O)₃(CO)₃]⁺ was acidified with 50 μ L concentrated HCl and then injected into a sealed vial containing 15 mg of NOHSO₄. After 10 min at 100 °C the reaction was cooled to room temperature and the pH adjusted to 6.5 with a 1/1 mixture of phosphate buffer and 10 N NaOH. The yield of the radioactive species [^{99m}TcCl(H₂O)₂(CO)₂NO]⁺ was >85% as evident from TLC analyses (Scheme 5). Remaining activity (<15%) was identified to be mainly ^{99m}TcO₄[−] and colloidal ^{99m}TcO₂. The stability of [^{99m}TcCl(H₂O)₂(CO)₂NO]⁺ at room temperature and acidic pH (1–6) was >90% during 1 half-life of the isotope. However, we observed rapid reoxidation of the product to [^{99m}TcO₄][−] at pH > 7.5. The characterization was accomplished chromatographically (HPLC) via comparison with the corresponding nonradioactive rhenium complex [ReCl(H₂O)₂(CO)₂NO]⁺ (see Supporting Information). Com-

plex $[^{99m}\text{TcCl}(\text{H}_2\text{O})_2(\text{CO})_2\text{NO}]^+$ reveals a retention time of 4.3 min and $[\text{ReCl}(\text{H}_2\text{O})_2(\text{CO})_2\text{NO}]^+$ showed a retention time of 4.2 min, whereas the starting materials $[^{99m}\text{Tc}(\text{H}_2\text{O})_3(\text{CO})_3]^+$ and $[^{99m}\text{TcO}_4]^-$ revealed retention times of 5.4 and 10.9 min, respectively. The preparation of the corresponding ^{188}Re precursor is currently in progress.

Conclusion

This work has shown the possibility of almost quantitative and selective formation of mixed dicarbonyl–nitrosyl complexes of technetium(I) and rhenium(I) in aqueous media. In the case of technetium a high tendency to form halide-bridged complexes was observed, whereas, in the case of rhenium, monomeric species can be isolated on the macroscopic level. Substitution of more than one CO ligand was not observed. Results of the density function calculations of complexes **4a** and **5** were in excellent agreements with the X-ray structural data and partially explained the selective

formation of single isomers. The possibility of production of the radioactive precursor $[^{99m}\text{TcCl}(\text{H}_2\text{O})_2(\text{CO})_2\text{NO}]^+$ in reasonable yields will allow the assessment of the potential of mixed carbonyl–nitrosyl organometallics of technetium-99m in radiopharmacy. Corresponding in vitro and in vivo experiments are currently in progress.

Acknowledgment. We thank Judith Stahel for her assistance in preparing the ^{99m}Tc complexes. This work was supported by Nihon MediPhysics.

Supporting Information Available: Data for structure solution and refinement, atomic coordinates, bond lengths and angles, and anisotropic thermal parameters for **3b**, **4a**, and **5** in CIF format, results of DFT calculations, and HPLC γ -traces and TLC γ -traces of complex $[^{99m}\text{TcCl}(\text{H}_2\text{O})_2(\text{CO})_2\text{NO}]^+$. This material is available free of charge via the Internet at <http://pubs.acs.org>.

IC049599K